[CANCER RESEARCH 61, 5382–5388, July 15, 2001]

Overexpression of Mitochondrial Manganese Superoxide Dismutase Protects against Radiation-induced Cell Death in the Human Hepatocellular Carcinoma Cell Line HLE[1]

Shigeatsu Motoori,[2] Hideyuki J. Majima,[3] Masaaki Ebara, Hirotoshi Kato, Futoshi Hirai, Shizuko Kakinuma, Chizuru Yamaguchi, Toshihiko Ozawa, Tetsuo Nagano, Hirohiko Tsujii, and Hiromitsu Saisho

Research Center of Charged Particle Therapy [S. M., H. K., F. H., H. T.], International Space Radiation Laboratory [H. J. M., S. K., C. Y.], Redox Research Group [T. O.], National Institute of Radiological Sciences, Chiba 263-8555, Japan; First Department of Medicine, Chiba University School of Medicine, Chiba, 260-0856, Japan [S. M., M. E., F. H., H. S.]; and Graduate School of Pharmaceutical Sciences, The University of Tokyo, Tokyo 113-0033, Japan [T. N.]

ABSTRACT

We investigated the potential role of mitochondrial manganese superoxide dismutase (Mn-SOD) in protective activity against irradiation by analyzing cell viability by a colony formation assay and by detecting apoptosis in stably human Mn-SOD gene-transfected HLE, a hepatocellular carcinoma cell line. We found that overexpression of Mn-SOD reduced the levels of reactive oxygen species in the mitochondria and intracellular phospholipid peroxidation product (4-hydroxy-2-nonenal) and prevented cell death. The production of intracellular nitric oxide after irradiation was not changed by Mn-SOD overexpression. The results suggested that Mn-SOD might play an important role in protecting cells against radiation-induced cell death by controlling the generation of mitochondrial reactive oxygen species and intracellular lipid peroxidation.

INTRODUCTION

ROS,[4] such as superoxide, hydrogen peroxide, and hydroxyl radicals, are molecules that contain oxygen and have higher reactivity than ground-state molecular oxygen. Ionizing radiation has been shown to generate ROS in a variety of cells (1). Recent evidence suggests that ROS play an important role in cell death and signal transduction by ionizing radiation (2). When water, the most copious intracellular material, is exposed to ionizing radiation, decomposition reactions occur, which form a variety of free radicals and molecular products (3). These products can peroxidize membrane lipids and attack proteins or DNA (4).

It has been proposed that, of these radicals, superoxide is a major factor in oxygen toxicity [superoxide theory of oxygen toxicity (5, 6)]. However, it has a limited reactivity with most biological molecules, raising questions about its toxicity *per se* (7). To account for the toxicity of superoxide *in vivo*, the secondary generation of a more reactive hydroxyl radical is proposed to occur by a superoxide-assisted Fenton reaction. The production of a hydroxyl radical by this reaction requires the interaction of superoxide, hydroxy peroxide, and suitably chelated iron, all kept at low concentrations *in vivo* because of efficient defense systems. Whereas the rate constant for the reduction of Fe^{3+} by the superoxide is only $1 \times 10^6\ M^{-1}\ s^{-1}$ (8), other cellular constituents, such as ascorbic acid, can reduce iron and are present in much higher concentrations than superoxide (9). Thus, the contribution of superoxide to hydroxyl radical production by the superoxide-assisted Fenton reaction may be limited *in vivo*, and other reactions may play important roles in superoxide toxicity.

Among other reactions, the reaction between superoxide radicals and NO to form peroxynitrite is a center of attention. Superoxide radicals can react with NO to form peroxynitrite in high yield because NO contains an unpaired electron and is paramagnetic (10). Peroxynitrite is a potent biological oxidant that has recently been implicated in diverse forms of free radical-induced tissue injury (11, 12). The reaction of peroxynitrite with membrane lipid induces a phospholipid membrane peroxidation product without requiring iron (13). A variety of aldehydes are generated as final products when lipid hydroperoxides break down. Among them, HNE is a highly toxic nine-carbon α,β-unsaturated aldehyde that can be generated by the peroxidation of ω6-unsaturated fatty acids, such as arachidonic and linoleic acid (14–16). In biological systems, HNE originates almost exclusively from phospholipid-bound arachidonic acid and may be the most reliable and sensitive marker of lipid peroxidation (14). *In vitro* studies have revealed that at relatively high concentrations, HNE causes rapid cell death associated with the depletion of sulfhydryl groups, disturbances in calcium homeostasis, inhibition of key metabolic enzymes, and inhibition of protein and DNA synthesis (14).

It is essential for aerobic organisms to possess enzymatic and nonenzymatic antioxidant defense systems that deal with ROS produced as a consequence of aerobic respiration. One important family of enzymes is the SOD (EC 1.15.1.1; Ref. 17). This family of enzymes is a class of metalloproteins that catalyzes the dismutation of superoxide radicals into hydrogen peroxide and molecular oxygen (5, 6). Hydrogen peroxide is further degraded to water by other antioxidant enzymes, such as glutathione peroxidase (EC 1.11.1.9) and catalase (EC 1.11.1.6). In mammalian cells, there are three types of SOD: (*a*) cytosolic Cu/Zn-SOD; (*b*) mitochondrial Mn-SOD (18); and (*c*) extracellular SOD (19). The biological importance of Mn-SOD is demonstrated by the following findings: (*a*) a lack of Mn-SOD genes in *Escherichia coli* and yeast makes them hypersensitive to oxidative stress (20–22); (*b*) homozygous mutant mice lacking Mn-SOD died within the first 10 days after birth and showed dilated cardiomyopathy, an accumulation of lipid in the liver and skeletal muscle, and metabolic acidosis (23); (*c*) mutant mice lacking Mn-SOD showed degenerative injury of large central nervous system neurons, particularly in the basal ganglia and brain stem, associated with damaged mitochondria and also showed progressive motor disturbances characterized by limb weakness, rapid fatigue, and circling behavior (24); (*d*) transfection of Mn-SOD cDNA into cultured cells rendered the cells resistant to paraquat (25)-, tumor necrosis factor (26, 27)-, doxorubicin (27)-, mitomycin C (27)-, radiation (27, 28)-, alkaline-(29)-, and cigarette smoke-induced cytotoxicity (30) and radiation-induced neoplastic transformation (31); and (*e*) the expression of

Received 11/14/00; accepted 5/9/01.

The costs of publication of this article were defrayed in part by the payment of page charges. This article must therefore be hereby marked *advertisement* in accordance with 18 U.S.C. Section 1734 solely to indicate this fact.

[1] Supported in part by Ground Research Announcement for Space Utilization promoted by Japan Space Forum and The Nuclear Cross-Over Research Study, Grant-in-Aid for Scientific Research (C) (2) 10671786 and 12671844 from the Ministry of Education, Culture, Sports, Science and Technology of Japan.

[2] Present adress: Department of Internal Medicine, Shimizu Kosei Hospital, Shizuoka 424-0114, Japan.

[3] To whom requests for reprints should be addressed, at International Space Radiation Laboratory, National Institute of Radiological Sciences, 4-9-1, Anagawa, Inage Ward, Chiba City, Chiba Pref. 263-8555, Japan. Phone: 81-43-206-3236; Fax: 81-43-251-4531; E-mail: hmajima@nirs.go.jp.

[4] The abbreviations used are: ROS, reactive oxygen species; NO, nitric oxide; DHR, dihydrorhodamine 123; HNE, 4-hydroxy-2-nonenal; SOD, superoxide dismutase; DAF, diaminofluorescein; DA, diacethyl; CCD, charge-coupled device; SF2, surviving fraction at 2 Gy.

Downloaded from http://aacrjournals.org/cancerres/article-pdf/61/14/5382/2862111/ch1401053382.pdf by guest on 11 November 2024

human Mn-SOD genes in transgenic mice protected the mice against oxygen-induced pulmonary injury (32) and Adriamycin-induced cardiac toxicity (33). Thus, the expression of Mn-SOD is essential for the survival of aerobic life and the development of cellular resistance to oxygen radical-mediated toxicity.

In this study, we examined the possible role of mitochondrial Mn-SOD in radiation-induced cell death. We report here that increased expression of mitochondrial Mn-SOD suppresses radiation-induced mitochondrial ROS generation and intracellular HNE production and also prevents nuclear condensation, DNA fragmentation, and cell death. Our results demonstrate that the production of mitochondrial ROS and intracellular HNE is an important mechanism by which radiation causes cellular lethality, suggesting that the removal of superoxide radicals by Mn-SOD in the mitochondria is a critical step in preventing radiation-induced cell death.

MATERIALS AND METHODS

Cell Lines. A human hepatocellular carcinoma cell line (HLE; Ref. 34) was purchased from the Health Science Research Resources Bank of Japan Health Sciences Foundation (Osaka, Japan). pCR3.1-Uni plasmid (Invitrogen, Carlsbad, CA) containing a sense human Mn-SOD cDNA insert was a kind gift of Dr. Makoto Akashi (National Institute of Radiological Sciences, Chiba, Japan). A sequence analysis of the Mn-SOD gene in the construct showed that the sequence was identical to that of accession number Y00472, except that C (nucleotide 113) was changed to T, and C (nucleotide 529) was changed to G, which make alanine to valine and glutamine to glutamic acid, respectively. The HLE cell line was transfected using the GenePORTER transfection procedure (Gene Therapy Systems, San Diego, CA) according to the manufacturer's instructions. Briefly, cells were plated 24 h before transfection at 60% confluence in a 60-mm dish. The cells were stably transfected with 6 μg of the pCR3.1-Uni plasmids containing a sense human Mn-SOD cDNA insert and linearized by *Sca*I in serum-free Dulbecco's Modified Eagle Medium (Life Technologies, Inc., Grand Island, NY). The controls were transfected with pCR3.1-Uni plasmids without human Mn-SOD cDNA insert and linearized by *Sca*I. Stable clones of both Mn-SOD and control plasmid transfectants were selected with Geneticin (Life Technologies, Inc.) at a final concentration of 500 μg/ml. Selected cellular clones that expressed Mn-SOD (Mn-SOD clones 6, 7, 10, and 13) or selectable marker alone (NEO-clones 1 and 2) and parental cells (HLE) were used in all experiments. Selected clones were routinely maintained in Dulbecco's Modified Eagle Medium containing 10% fetal bovine serum (JRH Biosciences, Lenexa, KS) and 500 μg/ml Geneticin at 37°C in humidified air containing 5% CO_2. Geneticin was removed at least 24 h before the experiments reported below were performed.

Irradiation. Each dish was irradiated to a dose of 15 Gy at room temperature using a Pantak 320S X-ray unit (Pantak Inc., East Haven, CT). The machine was operated at 200 kVp and 20 mA with a filter of 0.5 mm of Cu and 0.5 mm of Al. The dose rate was 1.0 Gy/min at a focus surface distance of 50 cm.

SOD Activity Gel Assay. A nondenatured gel assay for SOD activity was performed according to the method described previously (35), with slight modifications. Cells were sonicated in 50 mM potassium phosphate buffer (pH 7.8). A total of 50 μg protein/lane was electrophoresed through a nondissociating riboflavin gel consisting of 5% stacking gel (pH 6.8) and 12% running gel (pH 8.8) at 4°C. To visualize the SOD activity, gels were first incubated in 2.43 mM nitroblue tetrazolium (Wako Pure Chemical Industries, Ltd., Osaka, Japan) in deionized water for 20 min and then incubated in 0.028 mM riboflavin (Wako Pure Chemical Industries, Ltd.) and 280 mM *N,N,N′,N′*-tetramethylethylenediamine (Sigma Chemical Co., St. Louis, MO) in 50 mM potassium phosphate buffer (pH 7.8) for 15 min in the dark. Gels were then washed in deionized water and illuminated under fluorescent light until clear zones of SOD activity were evident. The images were obtained as TIFF files by a CCD camera in connection with Power Macintosh G3 (Apple Computer, Inc., Cupertino, CA). The bands of Mn-SOD were quantified by NIH Image 1.59, which is available on the internet via a file-transfer protocol.[5] Mn-SOD activity of the parental cell was normalized to 1, and the relative Mn-SOD activities of other cells were calculated. The mean of the integrated density obtained from the three independent files was used as a representative value for the experiment.

Cell Growth Assay. To determine the growth characteristics of the cells, they were plated in 60-mm tissue culture dishes at 5×10^4 cells/dish and cultured for 5 days. They were then trypsinized, and the number of cells was counted using a Coulter Z1 particle counter (Beckman Coulter, Fullerton, CA) daily. All experiments were repeated three times. The cell population doubling time was calculated as $0.693\ t/\ln(Nt/N_0)$ [t is time (in hours), Nt is the cell number at time t, and N_0 is the initial cell number].

Cell Survival Assay. Survival after irradiation was analyzed by *in vitro* colony formation. A stock culture near confluence was trypsinized, and the number of cells was counted by a Coulter Z1 particle counter (Beckman Coulter). One thousand cells were plated in plastic dishes. Twenty h after plating, the cells were irradiated and then returned to the incubator. After incubation at 37°C with 5% CO_2 for 13 days, the cells were stained with crystal violet, and colonies containing more than 50 cells were counted using a dissecting microscope. The surviving fraction was calculated by dividing the mean colony count at each radiation dose by the mean colony count of the unirradiated control group. Survival curves were plotted as the log of the surviving fraction of cells *versus* the radiation dose. All experiments were repeated three times.

Microscopic Assessment of Nuclear Chromatin Condensation and Fragmentation. Cells grown on glass-bottomed (35-mm) dishes (MatTek Corp., Ashland, MA) were stained with Hoechst 33342 fluorescent dye (Molecular Probes, Eugene, OR). Seventy-two h after irradiation, the cells were fixed for 30 min in a solution containing 4% formaldehyde in PBS and then incubated in PBS with 1 μg/ml dye for 30 min. The cells were washed twice with PBS and then washed twice with water. Fluorescence was visualized using an IX90 inverted microscope with an UPlanAPO ×20 objective lens (Olympus Optical Co., Tokyo, Japan). The dye was excited at 340 nm, and emission was filtered with a 510 nm barrier filter. Photographs of microscope fields were taken using a C5810-01 color chilled 3CCD camera (Hamamatsu Photonics K. K., Hamamatsu, Japan). More than 300 cells/culture dish were counted, and counts were made in three separate cultures per irradiation. Analyses were performed without knowledge of the irradiation history of the culture dishes. The percentage of apoptotic cells (apoptotic index) in each culture dish was determined.

Bioimaging of NO. DAFs (Daiichi Pure Chemicals, Tokyo, Japan) are fluorescent indicators for NO (36). They do not react with NO itself, but with NO+ equivalents, such as nitric anhydride (N_2O_3), which are produced by autooxidation of NO. DAF-FM DA, which was a kind gift from Daiichi Pure Chemicals, is a newly synthesized DAF that permeates well into cells and is quickly converted into water-soluble DAF-FM by esterases in the cytosol, where the dye can remain for a long time. Under aerobic conditions, DAF-FM traps NO to yield highly fluorescent triazofluoresceins by nitrosation and dehydration. Triazofluoresceins are not formed in the presence of NO. Glass-bottomed (35-mm) dishes (MatTek Corp.) with monolayers were prepared for staining with DAF-FM DA. One h after irradiation, the cell culture medium was replaced with modified HBSS containing 10.0 mM HEPES, 1.0 mM $MgCl_2$, 2 mM $CaCl_2$, and 2.7 mM glucose adjusted to pH 7.3 ± 0.05. Then, the cells were loaded with 10 μM DAF-FM DA by incubation for 30 min at 37°C. Bioimages of DAF-FM DA were acquired using a CSU-10 confocal laser scanning unit (Yokogawa Electric Co., Tokyo, Japan) coupled to an IX90 inverted microscope with UPlanAPO ×20 objective lens (Olympus Optical Co.) and a C5810-01 color chilled 3CCD camera (Hamamatsu Photonics K. K.). The DAF-FM DA was excited at 488 nm, and the emission was filtered using a 515 nm barrier filter. The intensity of the laser beam, the exposure time of the 3CCD camera, and the gain of the amplifier were held at 500 μW, 5 s, and 18 decibels, respectively, to allow quantitative comparisons of the relative fluorescence intensity of the cells between groups. Cells were chosen for analysis on a random basis and scanned twice. The values for the average fluorescence intensity/cell were obtained using IPLab Spectrum version 3.0 (Scanalystics Inc., Fairfax, VA) software with some modification of the program by the author (H. J. M.). The fluorescence intensity (which was acquired by confocal laser microscopy and analyzed by computer) after 15 Gy of irradiation divided by the intensity of sham-irradiated cells, *i.e.*, the relative fluorescence intensity, is calculated as the relative fluorescence intensity that

[5] http://rsb.info.nih.gov/nih-image/download.html.

Downloaded from http://aacrjournals.org/cancerres/article-pdf/61/14/5382/2862111/ch1401053382.pdf by guest on 11 November 2024

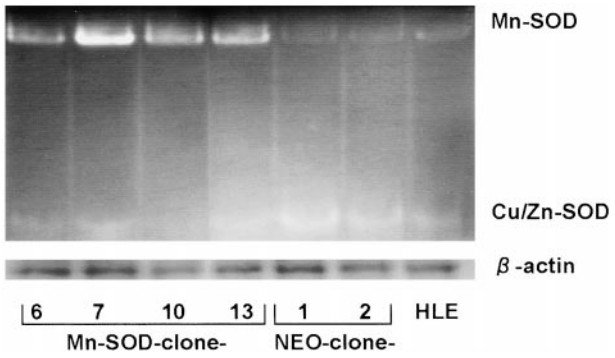

Fig. 1. Detection of Mn-SOD activity. Native polyacrylamide gel was stained for SOD activity in Mn-SOD clones 6, 7, 10, and 13; NEO clones 1 and 2; and HLE. Each lane was loaded with 50 μg of protein and electrophoresed through a 12% polyacrylamide gel at 4°C. Whereas the activity of Mn-SOD in parental cells and control plasmid transfectants was very low, the Mn-SOD activity in the Mn-SOD-transfected cells was clearly detectable.

Table 1 *Doubling time of the Mn-SOD-transfected clones, control plasmid transfectants, and parental cells*

Mn-SOD clone 6	35.6 ± 4.2 h
Mn-SOD clone 7	44.8 ± 1.6 h
Mn-SOD clone 10	25.8 ± 0.4 h
Mn-SOD clone 13	28.9 ± 0.7 h
NEO clone 1	25.7 ± 0.6 h
NEO clone 2	32.6 ± 1.3 h
HLE	32.7 ± 1.1 h

indicates the "increment" of the intensity induced by irradiation in each cell. Note that relative fluorescence intensity is *not* the ratio of the fluorescence intensity to the control plasmid-transfected cells or parental cells.

Relative Levels of Mitochondrial ROS. DHR (Molecular Probes) is an oxidation-sensitive lipophilic dye that enters a cell and fluoresces when oxidized by mitochondrial ROS to the positively charged rhodamine 123 derivatives. The relative level of mitochondrial ROS loaded with DHR was qualified by confocal laser microscope image using the same procedures described for DAF measurements, except that the final concentration of the dye used in the study was 10 μg/ml, and the exposure time of the 3CCD camera was 1.6 s.

Immunofluorescence Staining for HNE. Glass-bottomed (35-mm) dishes (MatTek Corp.) with monolayers were prepared for immunofluorescence staining with monoclonal antibody directed against proteins modified with the major membrane lipid peroxidation product, HNE. This monoclonal antibody (NOF Corp., Tokyo, Japan), which was specific for HNE-modified proteins, was raised by immunizing mice with a HNE-modified keyhole limpet hemocyanin conjugate (37). The antibody was tested for cross-reactivity toward glutaraldehyde, formaldehyde, 1-hexanal, 2-hexanal, 4-hydroxy-2-hexanal, and 2-nonenal. ELISAs with these potential competitors were performed. The results indicated that the anti-HNE antibody is highly specific to HNE-derived modifications to protein. Two h after irradiation, cells were fixed with 4% formaldehyde/PBS at room temperature for 30 min and rinsed twice with PBS, and membranes were permeabilized by incubation in 95% ethanol with 5% acetic acid for 10 min. After washing twice with PBS, cells were incubated for 4 min in a blocking serum (0.1% BSA in PBS) and incubated for 1 h in anti-HNE mouse monoclonal antibody at a dilution factor of 200. The cells were rinsed twice with 0.1% BSA in PBS and reincubated with Alexa Fluor 488 goat antimouse IgG (H+L) conjugate (Molecular Probes) for 1 h at room temperature. Image acquisition and analysis were similar to those of DAF-FM DA, except that the exposure time of the 3CCD camera was 5 s.

Statistical Analysis. A statistical analysis was performed by an ANOVA, followed by Fisher's *post hoc* tests. $P < 0.05$ was considered to be statistically significant. Data were presented as the mean ± SE. Calculations were performed with a statistical package, StatView 5.0J (SAS Institute Inc., Cary, NC), on a Power Macintosh G3 (Apple Computer, Inc.).

RESULTS

Isolation of HLE Transfectants Expressing Mn-SOD. The production of Mn-SOD activity in these transfectants was investigated in cell lysates (Fig. 1). The Mn-SOD activity of the parental cell line was normalized to 1, and the relative Mn-SOD activities of the other cells were calculated. The activity of Mn-SOD in HLE and NEO clone 1 and 2 cells was 1.0.97 ± 0.02 and 1.02 ± 0.13, respectively. The Mn-SOD activity in Mn-SOD clones 6, 7, 10, and 13 was clearly detectable, and the relative activities were 3.18 ± 0.33, 5.99 ± 1.10, 3.53 ± 0.36, and 3.18 ± 0.10, respectively, *i.e.*, the human Mn-SOD activity in the Mn-SOD-transfected cells was greater than that in the control cells. These results confirmed that (*a*) human Mn-SOD was not expressed much in the hepatocellular carcinoma cell line HLE, (*b*) but in the Mn-SOD-transfected cells, it remained stably expressed.

Doubling Time of the Cells. Table 1 shows the doubling time of the seven cell lines. The doubling times of the cells were not very different, except for that of Mn-SOD clone 7, which presented the strongest activity of Mn-SOD.

Morphology at the Light Microscopy Level. Cell morphology was detected by phase-contrast microscopy. The control cell typically showed an epithelial-like shape, whereas the Mn-SOD-transfected cells showed a long dendritic process (data not shown).

The Effect of Mn-SOD on Radiosensitivity. To determine the effect of radiation on cell survival, we performed an *in vitro* colony formation assay. Fig. 2 presents the survival curves of all cells used in the experiment irradiated with different doses of X-rays. The SF2

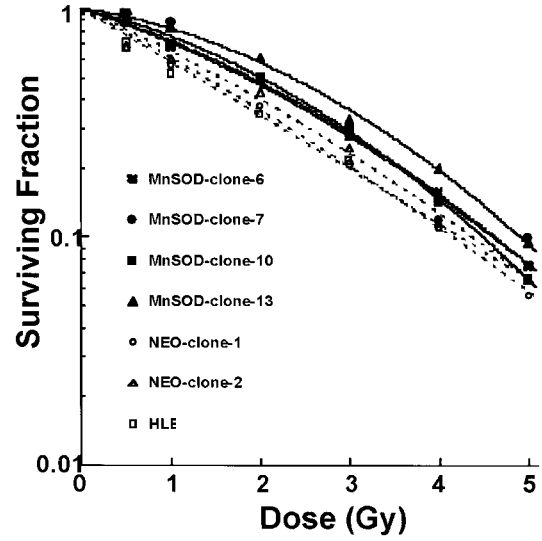

Fig. 2. Radiation survival curves for cells irradiated with 0–5 Gy of X-rays. After irradiations, cells were incubated for 13 days. Colonies containing more than 50 cells were counted and plotted as the log of the survival fraction of cells *versus* radiation doses. The curves were fitted by a linear quadratic equation, $S = e^{-(\alpha D + \beta D^2)}$, where S is the surviving fraction, and α and β are constants. *Points*, mean. *Solid lines*, Mn-SOD-transfected clones. *Dotted lines*, control plasmids transfectants and parental cells.

Table 2 *SF2 of the Mn-SOD-transfected clones, control plasmid transfectants, and parental cells*

Mn-SOD clone 6	0.50 ± 0.02[a]
Mn-SOD clone 7	0.50 ± 0.01[a]
Mn-SOD clone 10	0.50 ± 0.06[a]
Mn-SOD clone 13	0.62 ± 0.02[b]
NEO clone 1	0.38 ± 0.02
NEO clone 2	0.44 ± 0.02
HLE	0.35 ± 0.01

[a] $P < 0.01$ *versus* HLE, $P < 0.01$ *versus* NEO clone 1, NS *versus* NEO clone 2.
[b] $P < 0.0001$ *versus* HLE, $P < 0.0001$ *versus* NEO clone 1, $P < 0.001$ *versus* NEO clone 2.

Downloaded from http://aacrjournals.org/cancerres/article-pdf/61/14/5382/2862111/ch1401053382.pdf by guest on 11 November 2024

Table 3 *Absolute numbers of apoptotic cells and relative apoptotic index of the Mn-SOD-transfected clones, control plasmid transfectants, and parental cells*

Cell line	Apoptotic cell count after 15 Gy/0 Gy[a]	Relative apoptotic index
Mn-SOD clone 6	10.39/8.72	1.19 ± 0.24[b]
Mn-SOD clone 7	10.05/6.71	1.50 ± 0.15[c]
Mn-SOD clone 10	10.76/9.01	1.19 ± 0.23[b]
Mn-SOD clone 13	9.80/7.58	1.29 ± 0.14[d]
NEO clone 1	15.53/7.33	2.12 ± 0.11
NEO clone 2	17.50/9.06	1.93 ± 0.09
HLE	14.56/6.19	2.35 ± 0.10

[a] Absolute apoptotic cell number per 300 cells. Data shown on the table are average of three separate cultures.
[b] $P < 0.001$ *versus* HLE, $P < 0.01$ *versus* NEO clone 1, $P < 0.01$ *versus* NEO clone 2.
[c] $P < 0.01$ *versus* HLE, $P < 0.05$ *versus* NEO clone 1, $P = 0.0736$ *versus* NEO clone 2.
[d] $P < 0.001$ *versus* HLE, $P < 0.01$ *versus* NEO clone 1, $P < 0.05$ *versus* NEO clone 2.

Table 4 *Intracellular NO generation (relative fluorescence intensity) of the Mn-SOD-transfected clones, control plasmid transfectants, and parental cells*

Mn-SOD clone 6	1.21 ± 0.02
Mn-SOD clone 7	1.19 ± 0.00
Mn-SOD clone 10	1.25 ± 0.02
Mn-SOD clone 13	1.23 ± 0.01
NEO clone 1	1.24 ± 0.06
NEO clone 2	1.20 ± 0.03
HLE	1.21 ± 0.01

values are shown in Table 2. These two results show that compared with the parental cells and control plasmid transfectants, Mn-SOD-transfected clones were more resistant to irradiation.

The Effect of Mn-SOD on Radiation-induced Apoptotic Cell Death. To determine the effect of radiation on apoptotic cell death, we performed a microscopic assessment of nuclear chromatin condensation and a fragmentation assay using Hoechst 33342 staining. The percentage of apoptotic cells (apoptotic index) in each dish cultured for 72 h after irradiation was determined. The apoptotic index after 15 Gy of irradiation, which was divided by the apoptotic index of sham (0 Gy)-irradiated cells, *i.e.*, the relative apoptotic index, was calculated (see Table 3). The result shows that the relative apoptotic index was suppressed in the Mn-SOD-transfected cells compared with the HLE and NEO clones 1 and 2. This fact indicates that Mn-SOD suppresses radiation-induced apoptosis.

Mn-SOD Does Not Influence Radiation-induced NO Generation. To determine the effect of Mn-SOD on radiation-induced intracellular NO generation, DAF-FM DA, a dye sensitive to a change in the intracellular NO, was used. The dye was loaded 1 h after irradiation, and the images were acquired after 30 min of incubation. The fluorescence intensity (which was acquired by confocal laser microscopy and analyzed by computer) after 15 Gy of irradiation divided by the intensity on sham (0 Gy)-irradiated cells, *i.e.*, the relative fluorescence intensity, is shown in Table 4. This result shows that NO was almost equally increased at 15 Gy in all cells used in the experiment, indicating that Mn-SOD overexpression does not influence radiation-induced NO generation in the cell.

Mn-SOD Suppresses Radiation-induced Mitochondrial ROS Generation. To determine the effect of Mn-SOD on radiation-induced mitochondrial ROS generation, a dye sensitive to a change in the mitochondrial ROS was used. For an analysis of the levels of mitochondrial ROS, we used the same analytic technique used for NO. The dye was loaded 1 h after irradiation, and the images were acquired after 30 min of incubation. The relative fluorescence intensity is shown in Table 5. This result shows that the relative fluorescence intensity of DHR was depressed in the Mn-SOD-transfected cells compared with the HLE and NEO clones 1 and 2 cells, indicating that Mn-SOD suppresses radiation-induced ROS generation in the mitochondria.

Irradiation Induces Lipid Peroxidation. To determine whether changes in mitochondrial ROS generation are accompanied by an increase in the lipid peroxidation product, the levels of HNE were evaluated by immunohistochemical staining. The relative HNE staining intensity, which was obtained 2 h after irradiation, is shown in Table 6. This result shows that the relative HNE staining intensity was suppressed in the Mn-SOD-transfected cells compared with that in HLE and NEO clones 1 and 2, indicating that Mn-SOD suppresses the levels of the radiation-induced generation of intracellular HNE.

Correlation between Mitochondrial ROS, Intracellular Lipid Peroxidation Products, and Cell Death. To better understand the relationship between mitochondrial ROS, intracellular lipid peroxidation, and cell death, we used a scattergram to plot (*a*) the relative DHR staining intensity against the relative HNE staining intensity, (*b*) the relative HNE staining intensity against the relative apoptotic index, and (*c*) the relative HNE staining intensity against SF2, and then we analyzed the linear regression. Fig. 3*a* shows a linear regression analysis of the relative DHR staining intensity *versus* the relative HNE staining intensity ($r = 0.922$; $P = 0.0013$). Fig. 3*b* shows a linear regression analysis of the relative HNE staining intensity *versus* the relative apoptotic index ($r = 0.822$; $P = 0.0199$). These results show a strong positive correlation between the mitochondrial ROS, the intracellular lipid peroxidation products, and apoptosis. Fig. 3*c* illustrates a linear regression analysis of the relative HNE staining intensity *versus* SF2 ($r = -0.696$; $P = 0.0853$). Intracellular lipid peroxidation products have a strong correlation with apoptosis but a smaller correlation with the surviving fraction assessed by a colony formation assay.

DISCUSSION

In this study, the protective role of Mn-SOD against radiation injury was analyzed by using DHR fluorescence as a measure of ROS in mitochondria, immunohistochemical staining of HNE (a marker for lipid peroxidation), *in vitro* colony formation to examine cell viability, and Hoechst 33342 staining to detect apoptosis. Our results indicate that Mn-SOD seems to be an enzyme effective in protecting cells against ROS induced by ionizing radiation. Furthermore, the production of intracellular NO after irradiation was not suppressed by Mn-SOD.

In almost all aerobic cells, oxygen metabolism generates ROS, such

Table 5 *Mitochondrial ROS (relative fluorescence intensity) of the Mn-SOD-transfected clones, control plasmid transfectants, and parental cells*

Mn-SOD clone 6	1.01 ± 0.03[a]
Mn-SOD clone 7	0.99 ± 0.03[a]
Mn-SOD clone 10	1.02 ± 0.02[b]
Mn-SOD clone 13	1.03 ± 0.05[c]
NEO clone 1	1.25 ± 0.04
NEO clone 2	1.15 ± 0.02
HLE	1.16 ± 0.02

[a] $P < 0.01$ *versus* HLE, $P < 0.0001$ *versus* NEO clone 1, $P < 0.01$ *versus* NEO clone 2.
[b] $P < 0.01$ *versus* HLE, $P < 0.001$ *versus* NEO clone 1, $P < 0.01$ *versus* NEO clone 2.
[c] $P < 0.05$ *versus* HLE, $P < 0.001$ *versus* NEO clone 1, $P < 0.05$ *versus* NEO clone 2.

Table 6 *Intracellular HNE generation (relative fluorescence intensity) of the Mn-SOD-transfected clones, control plasmid transfectants, and parental cells*

Mn-SOD clone 6	1.03 ± 0.01[a]
Mn-SOD clone 7	1.02 ± 0.03[a]
Mn-SOD clone 10	0.99 ± 0.03[a]
Mn-SOD clone 13	1.03 ± 0.04[a]
NEO clone 1	1.26 ± 0.04
NEO clone 2	1.27 ± 0.01
HLE	1.15 ± 0.02

[a] $P < 0.01$ *versus* HLE, $P < 0.0001$ *versus* NEO clone 1, $P < 0.0001$ *versus* NEO clone 2.

Downloaded from http://aacrjournals.org/cancerres/article-pdf/61/14/5382/2862111/ch1401105382.pdf by guest on 11 November 2024

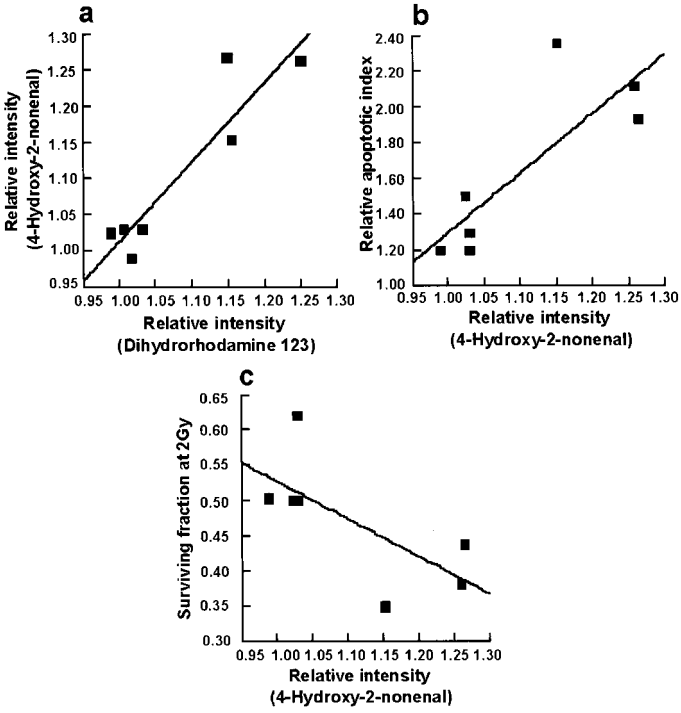

Fig. 3. Correlation between mitochondrial ROS, intracellular lipid peroxidation product, and cell death. *a*, linear regression analysis showing the relationship between the relative DHR staining intensity (mitochondrial ROS) and the relative HNE staining intensity (intracellular lipid peroxidation products) after irradiation ($r = 0.922$; $P = 0.0013$). *b*, linear regression analysis showing the relation between the relative HNE staining intensity and the relative apoptosis index ($r = 0.822$; $P = 0.0199$). *c*, linear regression analysis showing the relation between the relative HNE staining intensity and SF2 ($r = -0.696$; $P = 0.0853$). Intracellular lipid peroxidation products have a strong correlation with the apoptotic cell death but a smaller correlation with SF2, as assessed by colony formation.

as superoxide, hydroxyl radicals, and hydrogen peroxide. These ROS can peroxidize membrane lipids of a cell and organelles and can also attack DNA or protein (4). Among the various intracellular targets for ROS-mediated injury, mitochondria are thought to be particularly prone to ROS-induced damage (38). Because in most cells mitochondria consumes >95% of the cell's oxygen, the NADH-coenzyme Q reductase complex and the QH2 cytochrome *c* segment (cytochrome bc1 segment) of the mitochondrial electron transport chain are believed to be a principal source of endogeneous ROS generation. The electron transport chain yields electrons that produce a univalent reduction of oxygen to generate superoxide radicals (39). Mitochondrial DNA is highly sensitive to mutation by these endogenous ROS because mitochondrial DNA has no introns (making it more likely that a random mutation will strike a coding DNA sequence), no protective histones, and no effective DNA repair system (40). Mutations in any of the genes coding for cytochrome oxidase, cytochrome bc1, NADH dehydrogenase, or ATPase complexes may lead to an imperfect function of these enzymes. As a matter of course, under physiological conditions, only a small amount of oxygen consumed in mitochondria for respiration is changed into superoxide radicals (41). ROS production in mitochondria by ionizing radiation was apparently increased in control plasmid transfectants and parental cells as contrasted with Mn-SOD transfectants. There is a possibility that ROS generated by radiation in the mitochondria injure mitochondrial DNA and, as a result, lead to cell death. It has also been shown that ROS-generating alkylating toxins can cause mitochondrial DNA damage (42). Because SOD is specific for the elimination of superoxide radicals (6), our results also suggest that superoxide is the primary radical that leads to the increased amount of ROS detected.

Evidence has accumulated that mitochondria are major participants in apoptosis and that the ROS produced in mitochondria contribute to cell death by acting as apoptotic signaling molecules (43). Activators of apoptosis, such as caspase-2, caspase-9, cytochrome *c* (an activator of caspases), and apoptosis-inducing factor , all exist in mitochondria (44, 45). The release of cytochrome *c* (46, 47) and of apoptosis-inducing factor (44) from mitochondria is an irreversible implementation in the apoptotic process. Mitochondria also contain members of the Bcl-2 family, which regulates apoptosis (48). Overexpression of Bcl-2 prevented tumor necrosis factor-induced apoptosis and mitochondrial transmembrane potential, which is essential for mitochondrial function (49).

Recent studies suggest that the apoptosis of neuronal cells induced by oxidative stress is mediated by HNE, the major alkenal formed from oxidative degradation of membrane lipids (50); HNE can also directly mediate apoptotic and differentiating effects in K562 cells (51). Our study shows that the mitochondrial ROS, levels of HNE, and the apoptotic index are correlated with each other. There is a possibility that mitochondrial ROS form HNE and that this might help to release cytochrome *c* from the mitochondria and induce apoptosis. Mn-SOD might be able to prevent this course by reducing the production of mitochondrial ROS and HNE. Fig. 4 shows a schematic of the proposed hypothesis regarding how mitochondrial ROS and lipid peroxidation products accelerate cell death and the inhibition of cell death by Mn-SOD.

We note that in HLE and NEO clone 1 and 2 cells, the increase in the total intracellular HNE levels was correlated with increased mitochondrial ROS. Furthermore, in Mn-SOD-transfected cells, there was no measurable increase in the levels of both mitochondrial ROS and total intracellular HNE, suggesting that the removal of superoxide radicals in the mitochondria reduced the cellular oxidative stress at a distance from the mitochondria. A similar previous study (28) revealed that overexpression of human Mn-SOD protected against radiation-induced cell death, as assessed by a trypan blue dye exclusion test. The dead cell with a damaged cell membrane cannot exclude the trypan blue dye. This fact shows that although Mn-SOD exists in the mitochondria, it can protect the cell membrane. Why would the elimination of superoxide radicals in the mitochondria affect the levels of total cytosolic lipid peroxidation products? It is believed that in addition to its important role in respiration, mitochondrial respiration may also play a role in supporting the cellular redox status by decreasing cytosolic superoxide radicals (52). The cytosolic superoxide radical scavenging of mitochondria enhances the spontaneous dismutation of superoxide, which diffuses into the mitochondrial intermembrane space. The mitochondrial intermembrane space has a localized proton-rich condition that can protonate superoxide radicals to form hydroperoxyl radicals, which can then spread into mitochondrial matrices and are scavenged by Mn-SOD. Thus, superoxide

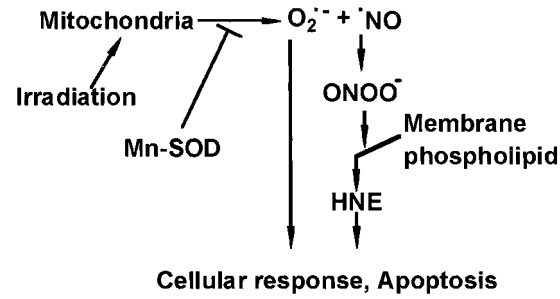

Fig. 4. Schematic diagram of a hypothesis on how ROS generation and lipid peroxidation products affect cell death and the prevention of cell death by Mn-SOD after irradiation.

Downloaded from http://aacrjournals.org/cancerres/article-pdf/61/14/5382/2862111/ch1401053382.pdf by guest on 11 November 2024

consumption in the mitochondria creates a gradient for superoxide radicals, which favors spreading from the cytosolic space to the mitochondrial space (52). For this reason, the removal of superoxide radicals from the mitochondria affects the levels of total cytosolic superoxide radicals and, as a result, the levels of lipid peroxidation products.

This is the first report of intracellular NO formation using a NO-detecting dye, DAF-FM DA, after irradiation. NO was produced homogeneously in the cell by irradiation according to an observation by confocal laser microscopy. In addition, the data indicated that Mn-SOD expression does not affect NO production. Similar previous research work was reported by Fricker *et al.* (53), who described the influence of SOD on NO production. The addition of SOD could not suppress the NO production of the RAW 264 macrophage, which was stimulated to produce NO by lipopolysaccharide and IFN-γ.

Superoxide can react with NO to form peroxynitrite and, in this way, can act as a mediator of ROS-mediated toxicity. The reaction of peroxynitrite with membrane lipid induces a membrane peroxidation product (13). The dye DHR was used to quantify the relative levels of mitochondrial ROS (54). DHR localizes to the mitochondria and fluoresces when oxidized to a positively charged rhodamine 123 derivative. Peroxynitrite is particularly effective in oxidizing DHR (55). For this reason, some investigators use this dye to measure the relative levels of peroxynitrite (12). Therefore, in our study, it is apparent that peroxynitrite has shown enhanced production in the mitochondria of control cells after irradiation. If cytosolic NO and cytosolic superoxide radicals form peroxynitrite, and this peroxynitrite induces membrane peroxidation, mitochondrial Mn-SOD cannot affect the total intracellular HNE. Therefore, there is a possibility that peroxynitrite was produced in the mitochondria and may diffuse to the cytosol and peroxidize the membrane lipids.

ACKNOWLEDGMENTS

We thank Dr. Makoto Akashi for MnSOD vectors and Dr. Daret K. St. Clair for helpful discussion.

REFERENCES

1. Riley, P. A. Free radicals in biology: oxidative stress and the effects of ionizing radiation. Int. J. Radiat. Biol., *65:* 27–33, 1994.
2. Schmidt-Ullrich, R. K., Dent P., Grant, S., Mikkelsen, R. B., and Valerie, K. Signal transduction and cellular radiation responses. Radiat. Res., *153:* 245–257, 2000.
3. Wallace, S. S. Enzymatic processing of radiation-induced free radical damage in DNA. Radiat. Res., *150* (Suppl. 5)*:* S60–S79, 1998.
4. Oxidative stress: adaptation, damage, repair and death. *In:* B. Halliwell and J. M. C. Gutteridge (eds.), Free Radicals in Biology and Medicine, 3rd ed., pp. 246–350. Oxford, United Kingdom: Oxford University Press, 1999.
5. Antioxidant defences. *In:* B. Halliwell and J. M. C. Gutteridge (eds.), Free Radicals in Biology and Medicine, 3rd ed., pp. 105–245. Oxford, United Kingdom: Oxford University Press, 1999.
6. Fridovich, I. Superoxide radical and superoxide dismutases. Annu. Rev. Biochem., *64:* 97–112, 1995.
7. Sawyer, D. T., and Valentine, J. S. How super is superoxide? Acc. Chem. Res., *14:* 393–400, 1981.
8. Winterbourn, C. C. Comparison of superoxide with other reducing agents in the biological production of hydroxyl radicals. Biochem. J., *182:* 625–628, 1979.
9. Babbs, C. F., and Griffin, D. W. Scatchard analysis of methane sulfinic acid production from dimethyl sulfoxide: a method to quantify hydroxyl radical formation in physiologic systems. Free Radic. Biol. Med., *6:* 493–503, 1989.
10. Blough, N. V., and Zafiriou, O. C. Reaction of superoxide with nitric oxide to form peroxynitrite in alkaline aqueous solution. Inorg. Chem., *24:* 3502–3504, 1985.
11. Beckman, J. S., Beckman, T. W., Chen, J., Marshall, P. A., and Freeman, B. A. Apparent hydroxyl radical production by peroxynitrite: implications for endothelial injury from nitric oxide and superoxide. Proc. Natl. Acad. Sci. USA, *87:* 1620–1624, 1990.
12. Keller, J. N., Kindy, M. S., Holtsberg, F. W., St. Clair, D. K., Yen, H. C., Germeyer, A., Steiner, S. M., Bruce-Keller, A. J., Hutchins, J. B., and Mattson, M. P. Mitochondrial manganese superoxide dismutase prevents neural apoptosis and reduces ischemic brain injury: suppression of peroxynitrite production, lipid peroxidation, and mitochondrial dysfunction. J. Neurosci., *18:* 687–697, 1998.
13. Radi, R., Beckman, J. S., Bush, K. M., and Freeman, B. A. Peroxynitrite-induced membrane lipid peroxidation: the cytotoxic potential of superoxide and nitric oxide. Arch. Biochem. Biophys., *288:* 481–487, 1991.
14. Esterbauer, H., Schaur, R. J., and Zollner, H. Chemistry and biochemistry of 4-hydroxynonenal, malonaldehyde and related aldehydes. Free Radic. Biol. Med., *11:* 81–128, 1991.
15. Pryor, W. A., and Porter, N. A. Suggested mechanisms for the production of 4-hydroxy-2-nonenal from the autooxidation of polyunsaturated fatty acids. Free Radic. Biol. Med., *8:* 541–543, 1990.
16. Spitz, D. R., Malcolm, R. R., and Roberts, R. J. Cytotoxicity and metabolism of 4-hydroxy-2-nonenal and 2-nonenal in H_2O_2-resistant cell lines. Do aldehydic by-products of lipid peroxidation contribute to oxidative stress? Biochem. J., *267:* 453–459, 1990.
17. McCord, J. M., and Fridovich, I. Superoxide dismutase. An enzymic function for erythrocuprein (hemocuprein). J. Biol. Chem., *244:* 6049–6055, 1969.
18. Weisiger, R. A., and Fridovich, I. Mitochondrial superoxide dismutase. J. Biol. Chem., *248:* 4793–4796, 1973.
19. Fukai, T., Siegfried, M. R., Ushio-Fukai, M., Cheng, Y., Kojda, G., and Harrison, D. G. Regulation of the vascular extracellular superoxide dismutase by nitric oxide and exercise training. J. Clin. Investig., *105:* 1631–1639, 2000.
20. Carlioz, A., and Touati, D. Isolation of superoxide dismutase mutants in *Escherichia coli*: is superoxide dismutase necessary for aerobic life? EMBO J., *5:* 623–630, 1986.
21. Farr, S. B., D'Ari, R., and Touati, D. Oxygen-dependent mutagenesis in *Escherichia coli* lacking superoxide dismutase. Proc. Natl. Acad. Sci. USA, *83:* 8268–8272, 1986.
22. van Loon, A. P. G. M., Pesold-Hurt, B., and Schatz, G. A yeast mutant lacking mitochondrial manganese-superoxide dismutase is hypersensitive to oxygen. Proc. Natl. Acad. Sci. USA, *83:* 3820–3824, 1986.
23. Li, Y., Huang, T-T., Carlson, E. J., Melov, S., Ursell, P. C., Olson, J. L., Noble, L. J., Yoshimura, M. P., Berger, C., Chan, P. H., Wallace, D. C., and Epstein, C. J. Dilated cardiomyopathy and neonatal lethality in mutant mice lacking manganese superoxide dismutase. Nat. Genet., *11:* 376–381, 1995.
24. Lebovitz, R. M., Zhang, H., Vogel, H., Cartwright, J., Jr., Dionne, L., Lu, N., Huang, S., and Matzuk, M. M. Neurodegeneration, myocardial injury, and perinatal death in mitochondrial superoxide dismutase deficient mice. Proc. Natl. Acad. Sci. USA, *93:* 9782–9787, 1996.
25. St. Clair, D. K., Oberley, T. D., and Ho, Y-S. Overproduction of human Mn-superoxide dismutase modulates paraquat-mediated toxicity in mammalian cells. FEBS Lett., *293:* 199–203, 1991.
26. Wong, G. H. W., Elwell, J. H., Oberley, L. W., and Goeddel, D. V. Manganous superoxide dismutase is essential for cellular resistance to cytotoxicity of tumor necrosis factor. Cell, *58:* 923–931, 1989.
27. Hirose, K., Longo, D. L., Oppenheim, J. J., and Matsushima, K. Overexpression of mitochondrial manganese superoxide dismutase promotes the survival of tumor cells exposed to interleukin-1, tumor necrosis factor, selected anticancer drugs, and ionizing radiation. FASEB J., *7:* 361–368, 1993.
28. Sun, J., Chen, Y., Li, M., and Ge, Z. Role of antioxidant enzymes on ionizing radiation resistance. Free Radic. Biol. Med., *24:* 586–593, 1998.
29. Majima, H. J., Oberley, T. D., Furukawa, K., Mattson, M. P., Yen, H-C., Szweda, L. I., and St. Clair, D. K. Prevention of mitochondrial injury by manganese superoxide dismutase reveals a primary mechanism for alkaline-induced cell death. J. Biol. Chem., *273:* 8217–8224, 1998.
30. St. Clair, D. K., Jordan, J. A., Wan, S., and Gairola, C. G. Protective role of manganese superoxide dismutase against cigarette smoke-induced cytotoxicity. J. Toxicol. Environ. Health, *43:* 239–249, 1994.
31. St. Clair, D. K., Wan, X. S., Oberley, T. D., Muse, K. E., and St. Clair, W. H. Suppression of radiation-induced neoplastic transformation by overexpression of mitochondrial superoxide dismutase. Mol. Carcinog., *6:* 238–242, 1992.
32. Wispe, J. R., Warner, B. B., Clark, J. C., Dey, C. R., Neuman, J., Glasser, S. W., Crapo, J. D., Chang, L-Y., and Whitsett, J. A. Human Mn-superoxide dismutase in pulmonary epithelial cells of transgenic mice confers protection from oxygen injury. J. Biol. Chem., *267:* 23937–23941, 1992.
33. Yen, H-C., Oberley, T. D., Vichitbandha, S., Ho, Y-S., and St. Clair, D. K. The protective role of manganese superoxide dismutase against Adriamycin-induced acute cardiac toxicity in transgenic mice. J. Clin. Investig., *98:* 1253–1260, 1996.
34. Doi, I., Namba, M., and Sato, J. Establishment and some biological characteristics of human hepatoma cell lines. Gann, *66:* 385–392, 1975.
35. Beauchamp, C., and Fridovich, I. Superoxide dismutase: improved assays and an assay applicable to acrylamide gels. Anal. Biochem., *44:* 276–287, 1971.
36. Kojima, H., Nakatsubo, N., Kikuchi, K., Kawahara, S., Kirino, Y., Nagoshi, H., Hirata, Y., and Nagano, T. Detection and imaging of nitric oxide with novel fluorescent indicators: diaminofluoresceins. Anal. Chem., *70:* 2446–2453, 1998.
37. Toyokuni, S., Miyake, N., Hiai, H., Hagiwara, M., Kawakishi, S., Osawa, T., and Uchida, K. The monoclonal antibody specific for the 4-hydroxy-2-nonenal histidine adduct. FEBS Lett., *359:* 189–191, 1995.
38. Wei, Y. H., Lu, C. Y., Lee, H. C., Pang, C. Y., and Ma, Y. S. Oxidative damage and mutation to mitochondrial DNA and age-dependent decline of mitochondrial respiratory function. Ann. N. Y. Acad. Sci., *20:* 155–170, 1998.
39. Beyer, R. E. An analysis of the role of coenzyme Q in free radical generation and as an oxidant. Biochem. Cell Biol., *70:* 390–403, 1992.
40. Bandy, B., and Davison, A. J. Mitochondrial mutations may increase oxidative stress: implications for carcinogenesis and aging? Free Radic. Biol. Med., *8:* 523–539, 1990.
41. Boveris, A., and Chance, B. The mitochondrial generation of hydrogen peroxide. General properties and effect of hyperbaric oxygen. Biochem. J., *134:* 707–716, 1973.

Downloaded from http://aacrjournals.org/cancerres/article-pdf/61/14/5382/2862111/ch1401053382.pdf by guest on 11 November 2024

42. Pettepher, C. C., LeDoux, S. P., Bohr, V. A., and Wilson, G. L. Repair of alkali-labile sites within the mitochondrial DNA of RINr 38 cells after exposure to the nitrosourea streptozotocin. J. Biol. Chem., *266:* 3113–3117, 1991.
43. Shimizu, S., Eguchi, Y., Kamiike, W., Matsuda, H., and Tsujimoto, Y. Bcl-2 expression prevents activation of the ICE protease cascade. Oncogene, *12:* 2251–2257, 1996.
44. Susin, S. A., Lorenzo, H. K., Zamzami, N., Marzo, I., Snow, B. E., Brothers, G. M., Mangion, J., Jacotot, E., Costantini, P., Loeffler, M., Larochette, N., Goodlett, D. R., Aebersold, R., Siderovski, D. P., Penninger, J. M., and Kroemer, G. Molecular characterization of mitochondrial apoptosis-inducing factor. Nature (Lond.), *397:* 441–446, 1999.
45. Susin, S. A., Lorenzo, H. K., Zamzami, N., Marzo, I., Brenner, C., Larochette, N., Prevost, M. C., Alzari, P. M., and Kroemer, G. Mitochondrial release of caspase-2 and -9 during the apoptotic process. J. Exp. Med., *189:* 381–394, 1999.
46. Yang, J., Liu, X., Bhalla, K., Kim, C. N., Ibrado, A. M., Cai, J., Peng, T. I., Jones, D. P., and Wang, X. Prevention of apoptosis by Bcl-2: release of cytochrome *c* from mitochondria blocked. Science (Wash. DC), *275:* 1129–1132, 1997.
47. Reed, J. C. Cytochrome *c*: can't live with it–can't live without it. Cell, *91:* 559–562, 1997.
48. Shimizu, S., Eguchi, Y., Kamiike, W., Waguri, S., Uchiyama, Y., Matsuda, H., and Tsujimoto, Y. Bcl-2 blocks loss of mitochondrial membrane potential while ICE inhibitors act at a different step during inhibition of death induced by respiratory chain inhibitors. Oncogene, *13:* 21–29, 1996.
49. Zamzami, N., Susin, S. A., Marchetti, P., Hirsch, T., Gomez-Monterrey, I., Castedo, M., and Kroemer, G. Mitochondrial control of nuclear apoptosis. J. Exp. Med., *183:* 1533–1544, 1996.
50. Kruman, I., Bruce-Keller, A. J. Bredesen, D., Waeg, G., and Mattson, M. P. Evidence that 4-hydroxynonenal mediates oxidative stress-induced neuronal apoptosis. J. Neurosci., *17:* 5089–5100, 1997.
51. Cheng, J-Z., Singhal, S. S., Saini, M., Singhal, J., Piper, J. T., Van Kuijk, F. J., Zimniak, P., Awasthi, Y. C., and Awasthi, S. Effects of mGST A4 transfection on 4-hydroxynonenal mediated apoptosis and differentiation of K562 human erythroleukemia cells. Arch. Biochem. Biophys., *372:* 29–36, 1999.
52. Guidot, D. M., Repine, J. E., Kitlowski, A. D., Flores, S. C., Nelson, S. K., Wright, R. M., and McCord, J. M. Mitochondrial respiration scavenges extramitochondrial superoxide anion via a nonenzymatic mechanism. J. Clin. Investig., *96:* 1131–1136, 1995.
53. Fricker, S. P., Slade, E., and Powell, N. A. Effect of superoxide dismutase on nitric oxide production by RAW264 macrophages. Biochem. Soc. Trans., *23:* 231S, 1995.
54. Mark, R. J., Keller, J. N., Kruman, I., and Mattson, M. P. Basic FGF attenuates amyloid β-peptide-induced oxidative stress, mitochondrial dysfunction, and impairment of Na^+/K^+-ATPase activity in hippocampal neurons. Brain Res., *756:* 205–214, 1997.
55. Kooy, N. W., Royall, J. A., Ischiropoulos, H., and Beckman, J. S. Peroxynitrite-mediated oxidation of dihydrorhodamine 123. Free Radic. Biol. Med., *16:* 149–156, 1994.

Downloaded from http://aacrjournals.org/cancerres/article-pdf/61/14/5382/2862111/ch1401053382.pdf by guest on 11 November 2024